Progress In Electromagnetics Research M, Vol. 47, 57–65, 2016

A Novel Smoothing Scheme of Temporal Basis Function Independent Method in MOT Based TDIE

Miao Miao Jia*, Yan Wen Zhao, Yu Teng Zheng, and Qiang Ming Cai

Abstract—In this paper, a novel numerical temporal convolution method is presented to calculate the convolutions between the retarded-time potentials and temporal basis functions (or its integration, derivation) in marching-on-in-time (MOT) solver. This approach can smooth and eliminate the singularity of integrated functions by variable substitution. It can also effectively control the precision of numerical quadratures over the surface of the source distribution. Thus it is suitable for more types of temporal basis functions, including non-piecewise polynomial functions. Numerical results demonstrate that this improved method can ensure the accuracy and late time stability of the MOT solver with different types of temporal basis functions.

1. INTRODUCTION

Time domain integral equation (TDIE) formulations have prevalent usage for analyzing broadband surface scattering phenomena, and the marching-on-in-time (MOT) method is a powerful tool for solving TDIE. However, the stability and accuracy of the MOT scheme are still challenging problems [1]. Many scholars have done many works in recent years and made very significant progress. Averaging/filtering scheme based on explicit MOT is considered to reduce the impact of the high frequency component on the late time stability [2–4]. However, these methods reduce the accuracy, increase the computation complexity and are invalid for large-scale and complex geometric structures. Later, implicit time stepping algorithms and appropriate smooth temporal basis functions are also proposed to overcome the above mentioned drawbacks [5–10]. Recent studies show that accuracy computation of the MOT impedance matrix is considered as a cure factor, effecting the late time stability and accuracy of the MOT solver [11–15].

On the other hand, a developed approach was proposed as shown in [16–19], which was different from the traditional MOT method. The spatial basis integral was performed first, and then the temporal convolution was evaluated, while the conventional MOT method was implemented in the reverse sequence. Firstly, exact closed-form expressions of the electric and magnetic fields and potentials due to impulsively excited Rao Wilton Glisson (RWG) basis functions have been presented in [19]. Secondly, analytical convolutions between some simple piece-wise polynomial's temporal basis functions $T(t)$ (or its derivation or integration) and retarded potentials (or its curl) have also been evaluated. However, the analytical integrals are heavily dependent on the expressions of $T(t)$. If some widely-used piecewise polynomials are used in modeling the temporal behavior of current, the convolution integrals can be calculated in a closed form. While the order of the polynomials is higher, the analytical expression is more complex, and more computing amounts are needed. Besides, if a non piece-wise polynomial temporal basis function is adopted [6, 20], the analytical result will be more complex or even cannot be derived. Thus a numerical convolution method is necessary. Since there still exist singularity in the integrated functions, the convergence will be poor using direct Gauss integrals [21].

Received 17 January 2016, Accepted 21 March 2016, Scheduled 25 March 2016

* Corresponding author: Miao Miao Jia (mmiaojia@126.com).

The authors are with the School of Electrical and Electronic Engineering, The University of Electronic Science and Technology of China, China.

To overcome the above drawbacks, a developed numerical convolution method is firstly applied to evaluate the convolutions. This proposed technique can eliminate the singularity (or smooth) of the integrated functions by introducing the idea of variable substitution [22, 23]. It is applicable to more types of $T(t)$ compared with the analytical convolution method [19]. Similarly, this idea has also been applied to solve the weakly and near singular problems existing in potential integrals for the frequency method [22].

This paper is organized as follows. Section 2 presents the formulation of MOT based time domain integral equation of PEC. Section 3 presents the evaluation of the improved temporal convolution method. Section 4 shows the numerical results that demonstrate the accuracy and stability of the proposed scheme. Section 5 presents conclusions.

2. FORMULATION OF MOT BASED TIME DOMAIN INTEGRAL EQUATION OF PEC

Suppose that S is the surface of the perfect electric conductor (PEC), the incident field $\mathbf{E}^{inc}(\mathbf{r},t)$ or $\mathbf{H}^{inc}(\mathbf{r},t)$ will generate induced current $\mathbf{J}_s(\mathbf{r},t)$ on the S and consequently generate the scattering field $\mathbf{E}^{sca}(\mathbf{r},t)$ or $\mathbf{H}^{sca}(\mathbf{r},t)$. According to the boundary conditions of electric and magnetic fields,

$$\hat{\mathbf{n}}\times\hat{\mathbf{n}}\times[\partial_t\mathbf{A}(\mathbf{r},t)+\nabla\Phi(\mathbf{r},t)] = \hat{\mathbf{n}}\times\hat{\mathbf{n}}\times\mathbf{E}^{inc}(\mathbf{r},t) \tag{1}$$

$$\mathbf{J}(\mathbf{r},t)-\hat{\mathbf{n}}\times\nabla\times\mathbf{A}(\mathbf{r},t) = \hat{\mathbf{n}}\times\mathbf{H}^{inc}(\mathbf{r},t) \tag{2}$$

where $\hat{\mathbf{n}}$ denotes the unit normal vector of field patch; $\mathbf{A}(\mathbf{r},t)$ and $\Phi(\mathbf{r},t)$ are the vector and scalar potentials; ∂_t denotes the time derivation; $\mathbf{E}^{inc}(\mathbf{r},t)$ and $\mathbf{H}^{inc}(\mathbf{r},t)$ denote the incident electric and magnetic fields, respectively.

In the MOT method, the unknown surface current density $\mathbf{J}(\mathbf{r},t)$ can be expanded as,

$$\mathbf{J}(\mathbf{r},t)=\sum_{n=1}^{N_s}\sum_{l=1}^{N_t}I_n^l\left[T_l(t)\mathbf{f}_n(\mathbf{r})\right] \tag{3}$$

where I_n^l are the unknown coefficients related to spatial basis functions $\mathbf{f}_n$ and temporal basis functions $T_l(t)=T(t-l\Delta t)(l=0,1,2,\ldots)$ (Δt denotes time step). Then using the point match at $t=k\Delta t$ in time domain, and adopting Galerkin methods in spatial domain, finally the time domain combined field integral equations (TDCFIE) can be divided into matrix equation,

$$\mathbf{M}_0^c\cdot\mathbf{I}^k=\mathbf{V}_k^{inc,c}-\sum_{l=1}^{k-1}\mathbf{M}_l^c\cdot\mathbf{I}^{k-l} \tag{4}$$

where

$$\mathbf{M}_l^c = \alpha_c\mathbf{M}_l^e+(1-\alpha_c)\eta\mathbf{M}_l^h \tag{5}$$

$$\mathbf{V}_k^{inc,c} = \alpha_c\mathbf{V}_k^{inc,e}+(1-\alpha_c)\eta\mathbf{V}_k^{inc,h} \tag{6}$$

where α_c denotes the weight coefficient of TDCFIE in time domain; $\alpha=1$ and $\alpha_c=0$ denote TDEFIE and TDMFIE, respectively; $\mathbf{V}_k^{inc,c}$ denotes the incident term caused by both $\mathbf{E}^{inc}(\mathbf{r},t)$ and $\mathbf{H}^{inc}(\mathbf{r},t)$; η is the wave impedance in free space; $\mathbf{M}_l^e$, $\mathbf{M}_l^h$ and $\mathbf{M}_l^c$ denote the matrix of TDEFIE, TDMFIE and TDCFIE, respectively. Their entries are,

$$M_l^e(m,n)=\int_{S_m}\mathrm{d}S\mathbf{f}_m(\mathbf{r})\cdot[\partial_t T(l\Delta t)*\mathbf{A}_n(\mathbf{r},t)]+\int_{S_m}\mathrm{d}S\nabla\cdot\mathbf{f}_m(\mathbf{r})\left[\partial_t^{-1}T(l\Delta t)*\phi_n(\mathbf{r},t)\right],\ l=0,1,\ldots \tag{7}$$

$$M_l^h(m,n)=\frac{T(l\Delta t)}{2}\int_{S_m}\mathrm{dS_m}\mathbf{f}_m(\mathbf{r})\cdot\mathbf{f}_n(\mathbf{r})-\int_{S_m}\mathrm{dS_m}\mathbf{f}_m(\mathbf{r})\cdot\hat{\mathbf{n}}_f\times\left[T(l\Delta t)*\mathbf{H}_n(\mathbf{r},t)\right],\ l=0,1,\ldots \tag{8}$$

where $\mathbf{f}_m(\mathbf{r})$ is the mth spatial testing function; $\hat{\mathbf{n}}_f$ is the normal unit vector of observation patch S_m; ∂_t and ∂_t^{-1} denote the derivative and integral of t, respectively; $\mathbf{A}_n(\mathbf{r},t)=\mathbf{A}_n^+(\mathbf{r},t)+\mathbf{A}_n^-(\mathbf{r},t)$, $\phi_n(\mathbf{r},t)=\phi_n^+(\mathbf{r},t)+\phi_n^-(\mathbf{r},t)$ and $\mathbf{H}_n(\mathbf{r},t)=\mathbf{H}_n^+(\mathbf{r},t)+\mathbf{H}_n^-(\mathbf{r},t)$ are the magnetic vector potential,

electric scalar potential and magnetic field due to impulsively excited nth basis function. The detailed expressions are as follows,

$$\mathbf{A}_n^{\pm}(\mathbf{r},t) = \frac{\mu}{4\pi}\int_{S_n^{\pm}} \mathrm{d}S'\mathbf{f}_{\mathbf{n}}(\mathbf{r}')\frac{\delta(t-R/c)}{R} = \pm\frac{cl_n}{2S_n^{\pm}}[\mathbf{e}^{\pm}(\mathbf{r},t)+(\rho-\rho_n^{\pm})\alpha^{\pm}(\mathbf{r},t)] \tag{9}$$

$$\phi_n^{\pm}(\mathbf{r},t) = \int_{S_n^{\pm}} \mathrm{d}S'\nabla'\cdot\mathbf{f}_{\mathbf{n}}(\mathbf{r}')\frac{\delta(t-R/c)}{R} = \pm\frac{cl_n}{S_n^{\pm}}\alpha(\mathbf{r},t) \tag{10}$$

$$\begin{aligned}\mathbf{H}_n{}^{\pm}(\mathbf{r},t) &= \int_{S_n^{\pm}} \mathrm{d}S'\nabla\times\left[\mathbf{f}_n(\mathbf{r}')\frac{\delta(t-R/c)}{R}\right] = \pm\frac{cl_n}{8\pi S_n^{\pm}}\hat{\mathbf{n}}\times(\rho-\rho_n^{\pm})\frac{1}{R}\frac{\partial\alpha(\mathbf{r},t)}{\partial R}|_{R=ct} \\ &\quad \mp\frac{cl_n}{8\pi S_n^{\pm}}\left[(\rho-\rho_n^{\pm})+d\hat{\mathbf{n}}\right]\times\frac{1}{R}\frac{\partial\mathbf{e}(\mathbf{r},t)}{\partial R}|_{R=ct}\end{aligned} \tag{11}$$

Here $S_n^{\pm}$ denotes the area of the source patch, c the velocity of the light in free space, l_n the length of the common edge of the nth basis function, and d the distance between the field point and the source triangle patch. It should be noted that all the related vectors are defined in the Cartesian local coordinate system, as shown in Fig. 1. $\alpha(\mathbf{r},t)$ and $\mathbf{e}(\mathbf{r},t)$ denote the arc length and bisecting vector of the arc formed by the intersection of the sphere and S_n, respectively. The closed-form expressions of $\alpha(\mathbf{r},t)$ and $\mathbf{e}(\mathbf{r},t)$ have been derived in details [17, 19].

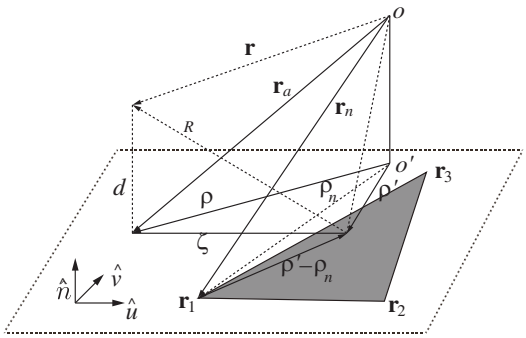

Figure 1. Cartesian local coordinate system and the related vector definition.

To complete the whole MOT solver, temporal convolutions between the potentials and the temporal basis functions have to be performed as indicated in Eqs. (7) and (8). However, it must be emphasized that the discontinuities in $\alpha(\mathbf{r},t)$ are very important and determinative for the singular behavior existing in Eqs. (9), (10) [16]. Similarly, the un-smooth property still exists in $\partial_R\alpha(\mathbf{r},t)$ or $\partial_R\mathbf{e}(\mathbf{r},t)$ in Eq. (11), which has singularity at tangent points [17]. Thus the direct numerical integration method is invalid in calculating the convolutions in Eqs. (7) and (8) due to its poor convergence. And a new smoothing scheme is required so as to guarantee fast convergence. In the next part, variable substitution is applied to eliminate the singularity or smooth the integrand of convolutions.

3. EVALUATION OF THE IMPROVED TEMPORAL CONVOLUTION METHOD

According to the analytical expressions of $\alpha(\mathbf{r},t)$ and $\mathbf{e}(\mathbf{r},t)$ [19], the convolutions of any temporal function with $\mathbf{A}_n(\mathbf{r},t)$, $\phi_n(\mathbf{r},t)$ and $\mathbf{H}_n(\mathbf{r},t)$ can be changed into calculating the convolutions between $F(t)$ and $T(t)$, namely, the temporal behavior of the impulsively excited electric field in EFIE or MFIE depends on those functions $F(t)$, given as shown in Table 1.

For better demonstration, $\widetilde{F}(t) = F(t) * T(t)$ is used to denote the convolution between the temporal basis $T(t)$ and $F(t)$. And one case of $F(t)$ is depicted to illustrate how the improved numerical convolutions work,

$$F(t) = 1/\sqrt{(ct)^2-d^2} \tag{12}$$

Table 1. The expression of $F(t)$ used in TDEFIE and TDMFIE ($\varsigma = \sqrt{c^2t^2 - d^2}$).

EFIE	1	ς	$\sqrt{\varsigma^2 - a_i^2}$	$\cos^{-1}(a_i/\varsigma)$
MFIE	$1/\varsigma$	$\sqrt{\varsigma^2 - a_i^2}/\varsigma^2$	$1/\varsigma^2\sqrt{\varsigma^2 - a_i^2}$	\

And the corresponding convolution is

$$\tilde{F}(t) = \int_{\tau_{\min}}^{\tau_{\max}} \left[\sqrt{(c\tau)^2 - d^2}\right]^{-1} T(t-\tau)d\tau \tag{13}$$

where $\tau_{\min}$ ($\tau_{\max}$) are the min (max) value of the radial integration interval, respectively. Here d is the distance of the observation point to the source path. Further, by making $x = c\tau$, we have

$$\tilde{F}(t) = \frac{1}{c}\int_{x_{\min}}^{x_{\max}} \left[\sqrt{x^2 - d^2}\right]^{-1} T(t - x/c)dx \tag{14}$$

It is easy to find that the integrated function does not continue when $x = d$, and the integrated function becomes large in their vicinity, thus reducing the accuracy and convergence of the numerical computation of the integral. we need to tackle the endpoint singularity of $\tilde{F}(t)$ if the lower limit of the segmented integration is $x_{\min} = d$. A considerable improvement of the behavior of the integrand function in the interval of integration is proposed by variable transformation,

$$x = d + y^q, \quad y = (x-d)^{1/q} \tag{15}$$

where q is a positive integer, and the integration variable is changed from x into y. Finally, we have

$$\tilde{F}(t) = \int_0^{(x_{\max}-d)^{1/q}} q\left[\sqrt{y^{2q} + 2dy^q}\right]^{-1} T(t - (d+y^q)/c)y^{q-1}dy \tag{16}$$

Therefore, the above mentioned singularity has been eliminated after variable substitution with the application of smoothing technique in Eq. (14) by changing the integration variable from x into y. Similarly, the same idea can be applied into solving all the other convolution integrals.

Taking the 1st order temporal basis function $T(t) = at + b$ for example and then putting it into Eq. (12), we have

$$\tilde{F}(t) = \int_{d/c}^{\tau_{\max}} \frac{a(t-\tau) + b}{\sqrt{(c\tau)^2 - d^2}}d\tau \tag{17}$$

where $\tau_{\max}$ is a constant bigger than d/c, and the related analytical and improved numerical expressions $\tilde{F}_A(t)$ and $\tilde{F}_N(t)$ are as follows,

$$\tilde{F}_A(t) = \frac{at+b}{c}\ln\left(c\tau + \sqrt{(c\tau)^2 - d^2}\right) - \frac{a}{c^2}\sqrt{(c\tau)^2 - d^2}\Big|_{d/c}^{\tau_{\max}} \tag{18}$$

$$\tilde{F}_N(t) = \frac{q}{c}\int_0^{y_{\max}} y^{q-1}\frac{-\frac{a}{c}y^q + (at + b - \frac{ad}{c})}{\sqrt{y^q(y^q + 2d)}}dy \tag{19}$$

where $y_{\max} = (c\tau_{\max} - d)^{1/q}$. In order to estimate the precision of our proposed numerical method, $E_r(t)$ is adopted to denote the relative error between $\tilde{F}_N(t)$ and $\tilde{F}_A(t)$,

$$E_r(t) = \frac{\tilde{F}_N(t) - \tilde{F}_A(t)}{\tilde{F}_A(t)} \tag{20}$$

If we choose $a = b = 1/\Delta t$, $d = 1$ and $\Delta t = 0.5\,\text{ns}$. $\tilde{F}(t)$ is calculated by traditional Gauss Legendre quadrature formula, analytical method and the proposed numerical method based on variable substitution, respectively. The relative error $E_r(t)$ with different q is shown in Fig. 2. The value of q can be confirmed by the requirement of calculating precision. When $q = 2$, the relative error (less than 10^{-6}) is the smallest among all results with q changing from 1 to 6. On the other hand, the results will not converge if using the direct Gauss Legendre quadrature method.

4. NUMERICAL RESULTS

Let's consider the PEC scatterers in the free space illuminated by the modulated plane-wave Gaussian pulse,

$$\mathbf{E}^{inc}(\mathbf{r},t) = \hat{\mathbf{p}}E_0 \cos\left[2\pi f_0\left(t - \mathbf{r}\cdot\hat{\mathbf{k}}\Big/c\right)\right] e^{-\left(t-t_p-\mathbf{r}\cdot\hat{\mathbf{k}}/c\right)^2\Big/(2\sigma^2)} \tag{21}$$

where E_0 and f_0 are the amplitude and center frequency of the incident wave. The temporal standard derivation $\sigma = 7/2\pi f_{bw}$. f_{bw} is the pulse width, and the delay relative to the origin is $t_p = 8\sigma$. $\hat{\mathbf{k}} = -\mathbf{e}_z$ denotes the propagation direction of the incident wave, and $\hat{\mathbf{p}} = \mathbf{e}_x$ denotes its polarization. $\mathbf{H}^{inc}(\mathbf{r},t) = \hat{\mathbf{k}} \times \mathbf{E}^{inc}(\mathbf{r},t)$. In this paper, four different types of $T(t)$ (1st and 2nd order Lagrange polynomials, sine, and exponential temporal basis functions) are adopted to examine and verify the accuracy and validity of the proposed method. $q = 2$ is chosen to guarantee the interpolation precision. Double-precision calculation and LU decomposition are also used in order to reduce the error of numerical truncation.

4.1. Analysis the Accuracy of This Numerical Time Convolution Method

In order to verify the accuracy and efficiency of the numerical temporal convolutions, the action between one field point and one source triangle path is given here. Three vertex coordinates of the source triangle S_n are $(-5.20, 6.14, 6.03)$, $(-8.61, 5.36, 12.17)$ and $(1.0, 1.732, 0.0)$, respectively. The field coordinate $\mathbf{r}$ is $(0.5, 2.0, 0.001)$ and time step $\Delta t = 0.25\,\text{ns}$. $\tilde{S}_e^1(\mathbf{r},t)$, $\tilde{V}_{e,u}^1(\mathbf{r},t)$ and $\tilde{V}_{h,u}^0(\mathbf{r},t)$ denote the convolutions between $\alpha(\mathbf{r},t)$ ($\mathbf{e}(\mathbf{r},t)$ or their derivation respect to R) and 1st temporal basis function (its derivation or integration respective to t), as shown at the bottom of Table 2. The detailed expression in the first

Table 2. The root mean square error between our proposed method and the analytical convolution method ($\times 10^{-6}$).

Δt (ns)	Gauss Node number	$\tilde{S}_e^1$ $(\mathbf{r},t)$	$\tilde{S}_e^{-1}$ $(\mathbf{r},t)$	$\tilde{\mathbf{V}}_{e,u}^1$ $(\mathbf{r},t)$	$\tilde{S}_h^0$ $(\mathbf{r},t)$	$\tilde{\mathbf{V}}_{h,u}^0$ $(\mathbf{r},t)$
1.0	3	0.271	3.621	1.306	0.345	0.250
1.0	5	1.748	2.927	0.969	0.171	0.270
1.0	7	1.173	8.185	0.636	0.302	0.313
0.5	3	2.511	4.743	1.814	0.321	0.549
0.5	5	1.860	3.061	0.980	0.378	0.370
0.5	7	1.462	1.327	1.050	0.328	0.380
0.25	3	1.889	6.117	1.605	0.596	1.067
0.25	5	1.985	3.861	1.093	0.481	0.604
0.25	7	1.758	5.534	1.115	0.480	0.604

line of Table 2 is as follows,

$$\tilde{S}_e^1(\mathbf{r},t) = \alpha(\mathbf{r},t) * \partial_t T(t) \tag{22}$$

$$\tilde{S}_e^{-1}(\mathbf{r},t) = \alpha(\mathbf{r},t) * \partial_t^{-1} T(t) \tag{23}$$

$$\tilde{\mathbf{V}}_{e,u}^1(\mathbf{r},t) = \mathbf{e}(\mathbf{r},t) * T(t) \tag{24}$$

$$\tilde{\mathbf{V}}_{h,u}^1 = -\partial_R e(\mathbf{r},t)/R * \partial_t T(t) \tag{25}$$

$$\tilde{S}_h^1 = -\partial_R \alpha(\mathbf{r},t)/R * \partial_t T(t) \tag{26}$$

For a better description, $f(t)$ is used to denote the above four convolutions uniformly. The root mean square error (RMS) between $f_N(t)$ (using our proposed method) and $f_A(t)$ (using analytical convolution method) is defined as

$$\mathrm{RMS} = \frac{\sum_{n=L_1}^{n=L_2} [\tilde{f}_N(n\Delta t) - \tilde{f}_A(n\Delta t)]^2}{L_2 - L_1 + 1} \tag{27}$$

Here t is changing from $t_1 = L_1\Delta t$ to $t_2 = L_2\Delta t$. L_1 and L_2 denote the L_1th and L_2th time steps, respectively. As shown in Table 2, the RMS is always less than 10^{-5} with different time steps and Gaussian integral nodes for both the convolutions used in TDEFIE and TDMFIE formulations.

4.2. Analysis Late-Time Stability and Accuracy of the MOT Algorithm with Different Temporal Basis Function

In this example, a PEC sphere with radius 0.5 m is considered. Its meshes include 458 planar triangular patches and 687 inner edges. The sphere is illuminated by a modulated Gaussian pulse with $f_0 = 200$ MHz and $f_{bw} = 80$ MHz. Fig. 3 shows a plot of current density amplitudes obtained from the proposed technique with four different temporal basis (TB) functions (as shown in Table 3) at the point $(0, 0, -1\,\mathrm{m})$. Here the time step Δt is equal to 0.36 ns. Three Gauss-Legendre points are used here. For TDCFIE ($\alpha_c = 0.2$) solver, the current density amplitudes match well with the result calculated by the analytical convolution (AC) solver with the 1st temporal basis function in all simulation times. For TDEFIE case, the current density amplitudes calculated by numerical convolution (NC) and AC agree well at early times. However, there is a gradual increase in its magnitude toward the end of simulation for the exponential temporal basis function.

Table 3. The expression of four different types of $T(\bar{\tau}\Delta t)$ ($\bar{\tau} = t/\Delta t$).

Types \ $\bar{\tau}$	$(-1, 0)$	$(0, 1)$	$(1, 2)$
1st	$1 + \bar{\tau}$	$1 - \bar{\tau}$	0
2nd	$1 + 1.5\bar{\tau} + 0.5\bar{\tau}^2$	$1 - \bar{\tau}^2$	$1 - 1.5\bar{\tau} + 0.5\bar{\tau}^2$
Sine	$1 - \sin^2(\pi\bar{\tau}/2)$	$1 - \sin^2(\pi\bar{\tau}/2)$	0
Exponential	$e^{-4.6487\bar{\tau}^2/(1+4\bar{\tau}^2-5\bar{\tau}^4)}$	$e^{-4.6487\bar{\tau}^2/(1+4\bar{\tau}^2-5\bar{\tau}^4)}$	0

In the second example, a cube of dimensions $1.0 \times 1.0 \times 1.0\,\mathrm{m}^3$ is meshed by planar triangle. The cube is partitioned into 680 triangular patches and 1020 unknowns. A modulated Gaussian pulse with $f_0 = 120$ MHz and $f_{bw} = 80$ MHz is incident on the cube. Here the time step Δt is equal to 0.25 ns. Similarly, we choose the above mentioned four different temporal basis functions. And three Gauss-Legendre points are adopted here. As shown in Fig. 4, the late time instability can be ensured using our proposed method for both the TDCFIE ($\alpha_c = 0.5$) and TDMFIE solvers. From Fig. 5, the bi-static RCS calculated by our proposed NC method agrees well with that of MOM in frequency domain.

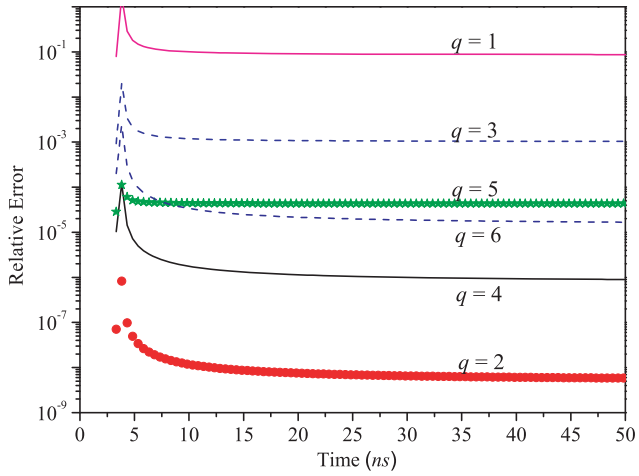

Figure 2. The relative error between the developed numerical method and analytical results with different q.

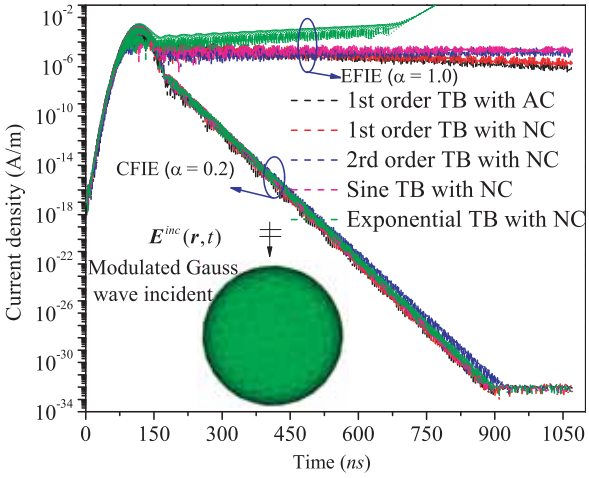

Figure 3. The magnitude of the current density for the sphere with different temporal basis functions.

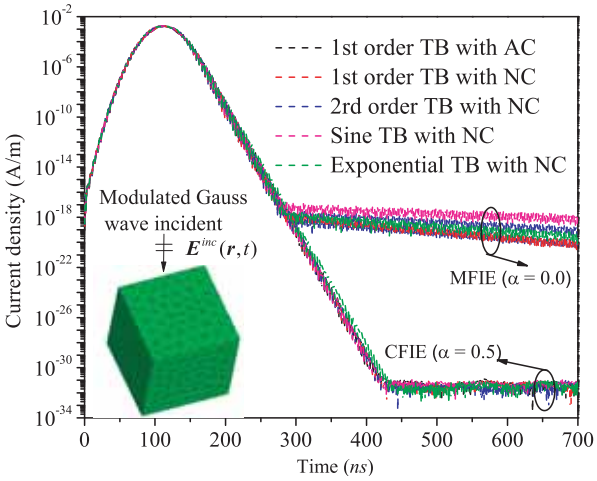

Figure 4. The magnitude of the current density for the cube with different temporal basis functions.

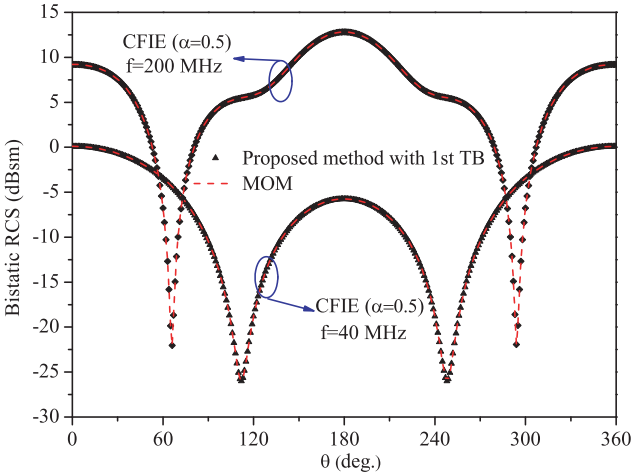

Figure 5. The Bi-static of the cube when the frequency equals to 40 MHz and 200 MHz.

5. CONCLUSION

Variable substitution is proposed to smooth and eliminate the singularity of the convolutions between the retarded potentials and the temporal basis functions. The calculating precision of our proposed method using different q is compared with the analytical results. As demonstrated by numerical examples, this improved numerical convolution method can ensure both the accuracy and the late time stability of the MOT algorithm with different types of temporal basis functions. Other types of time basis functions will be studied in future work.

REFERENCES

1. Shanker, B., A. A. Ergin, et al., "Analysis of transient electromagnetic scattering from closed surfaces using the combined field integral equation," *IEEE Trans. Antennas and Propag.*, Vol. 48, No. 7, 1064–1074, 2000.

2. Davies, P. J. and D. B. Duncan, "Averaging techniques for time-marching schemes for retarded potential integral equations," *Appl. Numer. Math.*, Vol. 23, No. 3, 291–310, 1997.
3. Vechinski, D. and S. M. Rao, "A stable procedure to calculate the transient scattering by conducting surfaces of arbitrary shape," *IEEE Trans. Antennas and Propag.*, Vol. 40, No. 6, 661–665, 1992.
4. Davies, P. J. and D. B. Duncan, "Averaging techniques for time-marching schemes for retarded potential integral equations," *Appl. Numer. Math.*, Vol. 23, No. 3, 291–310, 1997.
5. Dodson, S. J., S. P. Walker, and M. J. Bluck, "Implicit and stability of time domain integral equation scattering analysis," *Applied Computational Electromagnetic Society Journal*, Vol. 13, 291–301, 1997.
6. Weile, D. S., G. Pisharody, and N. W. Chen, "A novel scheme for the solution of the time-domain integral equations of electromagnetic," *IEEE Trans. Antennas and Propag.*, Vol. 52, No. 1, 283–295, 2004.
7. Wang, P., M. Y. Xia, J. M. Jin, and L. Z. Zhou, "Time-domain integral equation solvers using quadratic B-spline temporal basis functions," *Microw. Opt. Technol. Lett.*, Vol. 49, No. 5, 1154–1159, 2007.
8. Beghein, Y., K. Cools, H. Bagci, and D. De Zutter, "A space-time mixed galerkin marching on in time scheme for the time-domain combined field integral equation," *IEEE Trans. Antennas and Propag.*, Vol. 61, No. 3, 1228–1238, 2013.
9. Wildman, R. A., G. Pisharody, Weile, S. Daniel, S. Balasubramaniam, and E. Michielssen, "An accurate scheme for the solution of the time-domain Integral equations of electromagnets using higher order vector bases and bandlimited extrapolation," *IEEE Trans. Antennas and Propag.*, Vol. 52, No. 11, 2973–2984, 2004.
10. Bin Sayed, S., H. A. Ulku, and H. Bagci, "A stable marching on-in-time scheme for solving the time-domain electric field volume integral equation on high-contrast scatterers," *IEEE Trans. Antennas and Propag.*, Vol. 63, No. 7, 3098–3110, 2015.
11. Shi, Y. F., M. Y. Xia, R. S. Chen, E. Michielssen, and M. Y. Lu, "Stable electric field TDIE solvers via quasi-exact evaluation of MOT matrix elements," *IEEE Trans. Antennas and Propag.*, Vol. 59, No. 2, 574–585, 2011.
12. Pingenot, J., S. Chakraborty, and V. Jandhyala, "Polar integration for exact space-time quadrature in time-domain integral equations," *IEEE Trans. Antennas and Propag.*, Vol. 54, No. 10, 3037–3042, 2006.
13. Shanker, B., M. Lu, and E. Michielssen, "Time domain integral equation analysis of scattering from composite bodies via exact evaluation of radiation fields," *IEEE Trans. Antennas and Propag.*, Vol. 57, No. 5, 1506–1520, 2009.
14. Pray, A. J., N. V. Nair, and B. Shanker, "Stability properties of the time domain electric field integral equation using a separable approximation for the convolution with the retarded potential," *IEEE Trans. Antennas and Propag.*, Vol. 60, No. 8, 3772–3781, 2012.
15. Ulku, H. A., H. Bagci, and E. Michielssen, "Marching on-in-time solution of the time domain magnetic field integral equation using a predictor-corrector scheme," *IEEE Trans. Antennas and Propag.*, Vol. 61, No. 8, 4120–4131, 2013.
16. Yücel, A. C. and A. A. Ergin, "Exact evaluation of retarded-time potential integrals for the RWG bases," *IEEE Trans. Antennas and Propag.*, Vol. 54, No. 5, 1496–1502, 2006.
17. Ülkü, H. A. and A. A. Ergin, "Analytical evaluation of transient magnetic fields due to RWG current bases," *IEEE Trans. Antennas and Propag.*, Vol. 55, No. 12, 3565–3575, 2007.
18. Ülkü, H. A., A. A. Ergin, and T. Van, "On the singularity of the closed-form expression of the magnetic field in time domain," *IEEE Trans. Antennas and Propag.*, Vol. 59, No. 2, 691–694, 2011.
19. Ülkü, H. A. and A. A. Ergin, "Application of analytical retarded time potential expressions to the solution of time domain integral equation," *IEEE Trans. Antennas and Propag.*, Vol. 59, No. 11, 691–694, 2011.
20. Hu, J. L., C. H. Chan, and Y. Xu, "A new temporal basis function for the time-domain integral equation method," *IEEE Microw. Wireless Components Lett.*, Vol. 11, 465–466, 2001.

21. Ma, J., V. Rokhlin, and S. Wandzura, "Generalized Gaussian quadrature rules for systems of arbitrary functions," *SIAM Journal on Numerical Analysis*, Vol. 33, No. 3, 971–996, 1996.
22. Zhu, M. D., X. L. Zhou, and W. Y. Yin, "Radial integration scheme for handling weakly Singular and near-singular potential integrals," *IEEE Antennas and Wireless Propag. Letters*, Vol. 10, No. 1, 792–795, 2011.
23. Scuderi, L., "On the computation of nearly singular integrals in 3D BEM collocation," *International Journal for Numerical Methods in Engineering*, Vol. 74, 1733–1770, 2000.